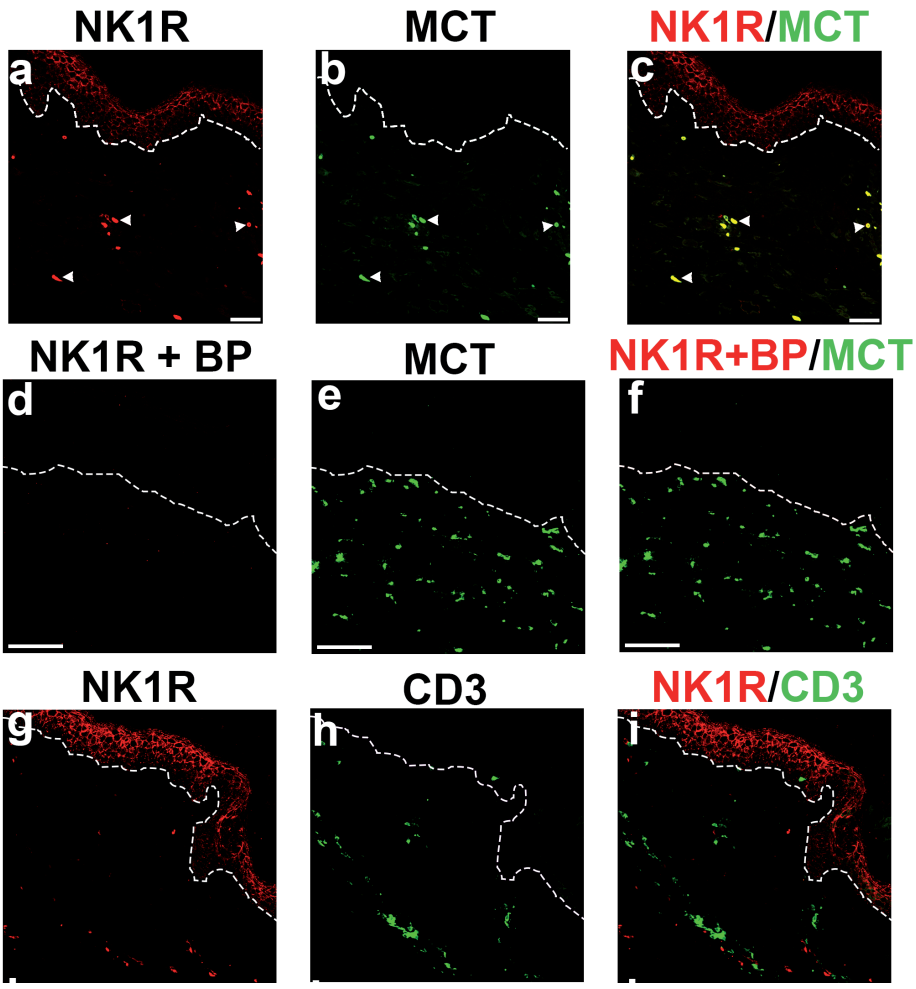

Fig. S1. Immunohistochemical expression of full-length NK1 receptor expression is blocked completely by immunizing peptide. Double immunohistochemical staining of 4 μm thick sections with NK1 Rc and mast cell tryptase (MCT) (a–c), NK1 Rc pre-absorbed with immunizing peptide and MCT (d–f), and NK1 Rc and CD3 (g–i). Arrowheads indicate mast cells (b) that co-label with NK1 Rc (a), shown as yellow (c), in human cutaneous scar. Pre-absorption with immunizing peptide completely abolishes NK1 Rc staining of keratinocytes and mast cells in human cutaneous scar (d–f). NK1 Rc is expressed in keratinocytes and mast cells but not CD3(+) cutaneous T cells in normal human skin (g–i). (c, f, i) Merged images of (a) & (b), (d) & (e), and (g) & (h), respectively. (a–i), × 200, dotted lines indicate the dermoepidermal junction. Scale bars, 50 μM.

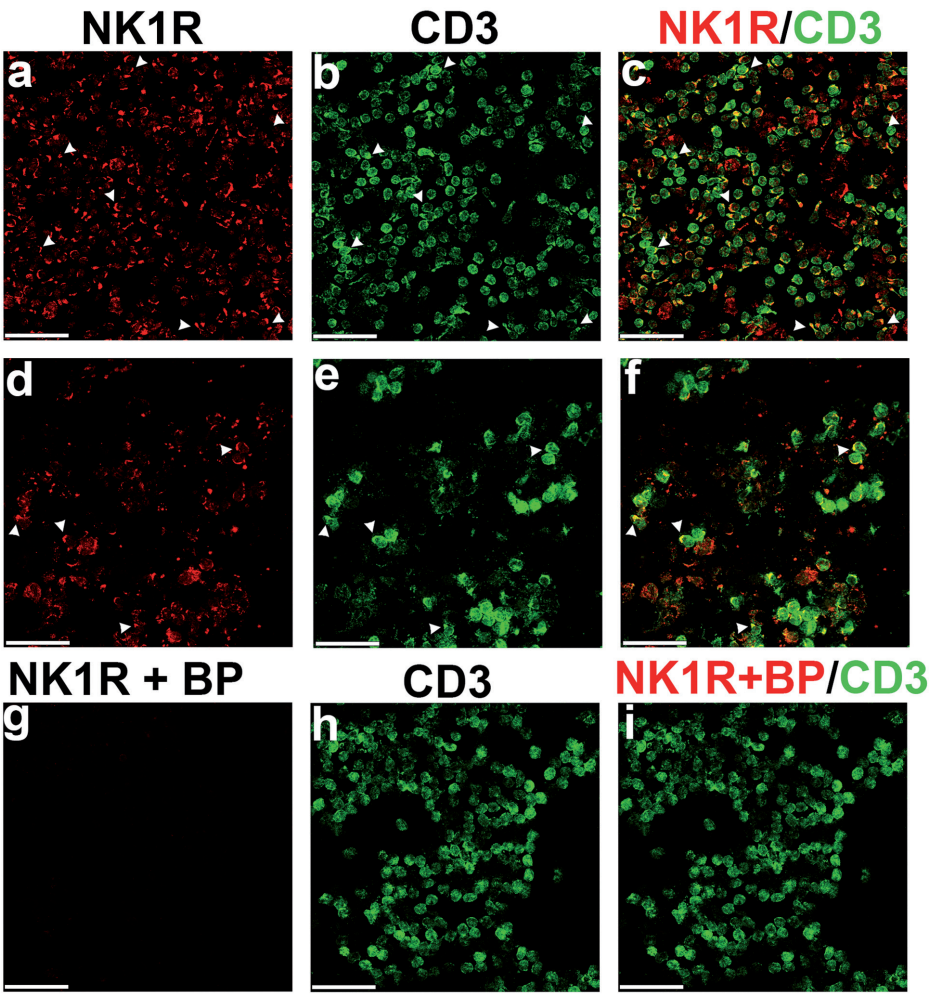

Fig. S2. Immunohistochemical expression of full-length NK1 receptor expression by circulating T cells in blood from controls and subjects with CTCL-MF. Double immunohistochemical staining with NK1 Rc and CD3 of peripheral blood monocytes from (a–c) a human control and (d–f) a CTCL-MF patient. (a–f) Arrowheads indicate circulating CD3(+) T cells (b, e) that co-label with NK1 Rc (a, d). (g–i) Double immunohistochemical staining with NK1R serum pre-absorbed with immunizing peptide and CD3, of peripheral blood monocytes from a human control. Pre-absorption with immunizing peptide completely abolishes NK1 Rc staining of circulated CD3(+) T cells. (c, f, i) Merged images of (a) & (b), (d) & (e), and (g) & (h), respectively. Co-labeling is shown as yellow. (a–i), ×400. Scale bars, 50 μM.

Appendix S1

SUPPLEMENTAL MATERIALS & METHODS AND RESULTS

Material

Subject sample and blood collection. Samples were obtained from cutaneous T-cell lymphoma patients from the Arizona Cancer Center (AZCC) and the Dana Farber Cancer Institute (DFCI), Harvard Medical School, Specialized Cutaneous Oncology Clinic. These subjects were originally recruited for a study correlating serum markers with disease stage and processed as described (S1). Healthy donors were recruited at Boston University Medical Center (BUMC). Specific information regarding demographics and characteristics of the disease were recorded prospectively. Characteristics of pruritus were not recorded prospectively. All protocols and procedures have been approved by the IRB committees at the BUMC, AZCC and the DFCI.

ELISAs. ELISAs were performed using the Quantikine Human SP Immunoassay kit (R&D Systems, Inc., Minneapolis, MN), according to manufacturer's protocols. The optical density at 450-570 nm was measured with a VMax kinetic Microplate reader (Molecular Devices, Sunnyvale, CA). The final concentrations of SP in plasma were calculated based on standard curve values.

Immunohistochemistry on slide-mounted sections. Following approval by the IRB at Boston University, paraffin-embedded skin biopsies from 17 CTCL-mycosis fundiodes (CTCL-MF) patients, normal skin, and from scars obtained from otherwise healthy individuals, were obtained. 11 of the 17 CTCL-MF samples had accessible medical records that were reviewed to determine if the skin lesion sampled had definitive evidence of pruritus at the time of biopsy. Five of 17 had definitive evidence of active pruritus in the lesion biopsied at the time of biopsy. Of the remaining 12 CTCL-MF biopsies, active but undocumented pruritus may have existed, as 66% to 88% of CTCL-MF patients have reported pruritus {Vij, 2012 #17}. All samples were sectioned at 4 μM, deparaffinized with HistoClear solution (National Diagnostics, Atlanta, GA), rehydrated, antigen unmasked (95oC for 40 min in pH=9.0 buffer from Vector Labs, Burlingame, CA), peroxidase quenched, incubated in primary antibody at +4°C overnight and secondary antibody for 1 h at room temperature. Enzymatic detection used either tyramide-Alexa Fluor 488 or tyramide-Alexa Fluor 568 (Life Technologies). For double-labeling experiments, residual HRP activity was inactivated by 30 min incubation in 27% H202/1XPBS/0.25% triton-X solution. Sections were blocked again for 1 h, and the antibody staining procedure repeated.

Primary antibodies. C-terminus-detecting primary NK1R antibody (detects full-length NK1R only) used for the experiments in this paper: rat-anti-human NK1R (Immunostar, #20060; 1:1000). This well-characterized antibody is raised against a peptide sequence at the carboxy C-terminus of rat NK1 receptor (residues 393–407: KTMTESSSFYSNMLA). This antiserum detected NK1R only in a cell line transfected with a chimeric NK1 receptor construct but not vector alone and to give an expression pattern in rat brain that highly correlated with both 125I-labeled NK1 receptor-binding sites and autoradiographic localization of 3H-substance P (S2). Immunolabeling was absent in NK1R-deficient knock-out mice (S2). Preadsoprtion with the immunizing peptide abolished immunolabeling in rat and normal human brain sections and Western blots of rat brain tissue (antibody data sheet, Immunostar) (S2).

N-terminus-detecting primary NK1R antibody (would detect both full-length and truncated NK1R) used only in preliminary optimization trials, including reproducing the conditions of Remröd et al. (S3): Novus Biologicals, NB300-119. Other non-NK1R primary antibodies used: mouse-anti-human CD3 (clone F7.2.38, DAKO, M7254; 1:875), and mouse anti-mast cell tryptase (clone AA1, Abserotec, MCA1438T; 1:200).

Secondary antibodies: ImmPress (Vector Labs) for CD3 and NK1R or donkey anti-mouse dyL488 (Jackson Immunoresearch, West Grove, PA).

For peptide blocking experiments, the primary antibody solution was pre-incubated 16 hours at +4°C with the immunizing peptide (Immunostar, #24340) at 20 μG/ml.

Immunohistochemistry on cytospin preparations. Cytospins of blood cells were prepared and stained with immunohistochemical buffers and antibodies using the same antibody reagents and concentrations as per the paraffin sections above. The nuclei were counterstained with SlowFade Gold anti-fade reagent with DAPI (Invitrogen Molecular Probes, Eugene, OR). All image analyses were performed with Zeiss Axioskop 40 microscope (Carl Zeiss MicroImaging, LLC., Thornwood, NY), using the Axiovision Rel. 4.6 software (×400 magnified).

Immunohistochemistry on free-floating sections. 50 μM thick rolls were cut from 9 of the 17 randomly selected CTCL-MF paraffin blocks, deparaffinized by standard procedures and subjected, without antigen retrieval, to triple-label free floating immunohistochemistry as described (2) using guinea pig anti-substance P (1:12,000; Neuromics, Edina, MN), mouse-anti-human CD3 (clone F7.2.38, DAKO, M7254; 1:875), and rabbit anti-protein gene product 9.5 (1:18,000; AbSerotec, Raleigh, NC) as primaries; using donkey anti-guinea pig, anti-rabbit HRP, or anti-mouse HRP (Jackson Immunoresearch, West Grove, PA) as secondaries; and tyramide amplification (Life Technologies).

Quantitation of nerve length in free-floating sections. For each specimen, two or three 2.4 mm wide fields containing SP+ nerves were selected, each corresponding to a different tissue piece from a bi- or tri-sected biopsy section. Images were acquired at 4 μm intervals throughout the depth of the specimen for the entire 2.4 mm wide field using a ×20 lens (Z-series), separately for each fluorescent signal. In all cases, the imaging field had at its most rostral edge, the stratum corneum and extended to a depth of at least 200 μm beneath the dermal-epidermal junction visible using endogenous autofluorescence of keratinocytes. Image J (NIH) and Neuron J (S4) software were used to quantitate nerve lengths as previous described (2). JMP10 statistical software was used to calculate percentages of nerve fibers, presented as median with 25% and 75% quartiles. Statistical analyses were performed with one-way ANOVA analysis and either Dunnett's, or Mann-Whitney post-test. $p < 0.05$ was considered significant.

Results

We performed preliminary experiments to optimize immunohistochemical staining of both the C-terminus-directed and N-terminus-directed NK1R primary antibodies. The expression pattern generated by the C-terminus antibody (fl-NK1R) correlated with findings from previously reported studies that used either biotinylated or I-125-conjugated SP on frozen sections or used immunohistochemistry on formalin-fixed sections with an antibody targeting the N-terminus of the NK1R (9, S3, S5, S6). In normal skin, surgically-induced scars, and in five randomly selected CTCL-MF skin samples, we confirmed the dermal fl-NK1R expressing cells were mast cells, using double-immunohistochemical labeling with mast-cell tryptase (Fig. S1[1] and data not shown). Fl-NK1R staining was abolished when the C-terminal primary antibody was omitted or when this primary antibody was pre-incubated with the immunizing peptide in skin (Fig. S1[1]) and in cytospin samples (Fig. S2[1]). These experiments confirmed the specificity of the staining in human skin and blood samples. The N-terminus antibody

produced only non-specific staining (data not shown). Therefore, only the C-terminus antibody was used for subsequent immunohistochemical detection of fl-NK1r.

SUPPLEMENTAL REFERENCES

S1. Richmond J, Tuzova M, Parks A, Adams N, Martin E, Tawa M, et al. Interleukin-16 as a marker of Sezary syndrome onset and stage. J Clin Immunol 2011; 31: 39–50.

S2. Lessard A, Coleman CG, Pickel VM. Chronic intermittent hypoxia reduces neurokinin-1 (NK(1)) receptor density in small dendrites of non-catecholaminergic neurons in mouse nucleus tractus solitarius. Exp Neurol 2010; 223: 634–644.

S3. Remröd C, Lonne-Rahm S, Nordlind K. Study of substance P and its receptor neurokinin-1 in psoriasis and their relation to chronic stress and pruritus. Arch Dermatol Res 2007; 299: 85–91.

S4. Meijering E, Jacob M, Sarria JC, Steiner P, Hirling H, Unser M. Design and validation of a tool for neurite tracing and analysis in fluorescence microscopy images. Cytometry A 2004; 58: 167–176.

S5. Staniek V, Liebich C, Vocks E, Odia SG, Doutremepuich JD, Ring J, et al. Modulation of cutaneous SP receptors in atopic dermatitis after UVA irradiation. Acta Derm Venereol 1998; 78: 92–94.

S6. Toyoda M, Nakamura M, Nakada K, Nakagawa H, Morohashi M. Characteristic alterations of cutaneous neurogenic factors in photoaged skin. Br J Dermatol 2005; 153: Suppl 2: 13–22.

Table SI. *Demographics of cutaneous T-cell lymphoma-mycosis fungoides patients for immunohistochemistry experiments*

Age, years/ Sex	Race	Anatomic region	Grouped stage[a]	Known pruritus	Slide staining	Free floating sections
50/M	C	Trunk	Early	Yes	Yes	Yes
48/M	C	Extremity	Early	Yes[b]	Yes	Yes
54/M	C	Trunk	Early	Unknown	Yes	Yes
77/F	C	Extremity	Later	Yes[b]	Yes	Yes
68/M	N/A	Trunk	Early	N/A	Yes	Yes
78/M	C	Trunk	Early	N/A	Yes	Yes
39/F	AA	Extremity	Early	Unknown	Yes	Yes
63/M	N/A	Trunk	Early	N/A	Yes	Yes
60/M	C	Trunk	Later	Yes	Yes	Yes
56/F	N/A	Trunk	Early	N/A	Yes	No
72/M	C	Trunk	Later	Yes	Yes	No
72/F	C	Head/neck/scalp	Early	Yes[b]	Yes	No
68/M	AA	Trunk	Later	Yes[b]	Yes	No
88/M	C	Trunk	Early	N/A	Yes	No
63/M	C	Trunk	Early	Yes[b]	Yes	No
73/M	C	Extremity	Early	Unknown	Yes	No
35/M	CV	Extremity	Early	Unknown	Yes	No

[a]Early: Stages IA and IB; Later: Stages IIA-IVB. [b]Pruritus documented to be present from lesion biopsied.
C: Caucasian; N/A: No chart available; AA: African-American; CV, Cape Verdian.

Table SII. *Demographics of subjects for ELISA measurement of serum substance P (SP) levels and cytospin immunohistochemistry*

	Normals ($n=4$)	Early stages CTCL-MF ($n=19$)*	Later stages CTCL-MF ($n=15$)*
Age, years, mean, SD	52.3, 18.6	58.2, 13.6	70.8, 11.3
Male, *n*	4	12	9
Female, *n*	0	7	6

Early: Stages IA and IB; Later: Stages IIA-IVB.
CTCL-MF: cutaneous T-cell lymphoma-mycosis fungoides.